



Deterioration of bone microstructure by aging and menopause in Japanese healthy women: analysis by HR-pQCT

Kazuaki Yokota¹ · Ko Chiba¹ · Narihiro Okazaki¹ · Choko Kondo¹ · Mitsuru Doi¹ · Shuta Yamada¹ · Makoto Era¹ · Yuichiro Nishino¹ · Akihiko Yonekura¹ · Masato Tomita¹ · Makoto Osaki¹

Received: 11 January 2020 / Accepted: 14 May 2020 / Published online: 9 June 2020
© The Japanese Society Bone and Mineral Research and Springer Japan KK, part of Springer Nature 2020

Abstract

Introduction Second-generation high-resolution peripheral quantitative computed tomography (HR-pQCT) has provide higher quality of bone images with a voxel size of 61 μm , enabling direct measurements of trabecular thickness. In addition to the standard parameters, the non-metric trabecular parameters such as trabecular morphology (plate to rod-like structures), connectivity, and anisotropy can also be analyzed. The purpose of this study is to investigate deterioration of bone microstructure in healthy Japanese women by measuring standard and non-metric parameters using HR-pQCT.

Materials and methods Study participants were 61 healthy Japanese women (31–70 years). The distal radius and tibia were scanned using second-generation HR-pQCT, and microstructures of trabecular and cortical bone were measured. Non-metric trabecular parameters included structure model index (SMI), trabecular bone pattern factor (TBPf), connectivity density (Conn.D), number of nodes (N.Nd/TV), degree of anisotropy (DA), and star volume of marrow space ($V^*\text{ms}$). Estimated bone strength was evaluated by micro finite element analysis. Associations between bone microstructure, estimated bone strength, age, and menopause were analyzed.

Results Trabecular number declined with age, and trabecular separation increased. SMI and TBPf increased, Conn.D and N.Nd/TV declined, and $V^*\text{ms}$ increased. Cortical BMD and thickness declined with age, and porosity increased. Stiffness and failure load decreased with age. Cortical thickness and estimated bone strength were affected by menopause. Cortical thickness was most associated with estimated bone strength.

Conclusions Trabecular and cortical bone microstructure were deteriorated markedly with age. Cortical thickness decreased after menopause and was most related to bone strength. Non-metric parameters give additional information about osteoporotic changes of trabecular bone.

Keywords High resolution peripheral quantitative CT (HR-pQCT) · Bone microstructure · Estimated bone strength · Non-metric trabecular parameter · Japanese women

Introduction

Dual-energy X-ray absorptiometry (DXA) is widely used in the risk assessment of fragility fracture and diagnosis of osteoporosis. However, DXA evaluates bone in two

dimensions, being difficult to use for separate evaluation of cortical and trabecular bone or analysis of bone microstructure [1, 2].

High-resolution peripheral quantitative computed tomography (HR-pQCT) was developed in 2004, allowing an in vivo analysis of the microstructures of human cortical and trabecular bone separately in three dimensions [3–5]. With the advent of second-generation HR-pQCT in 2014, voxel size improved from 82 to 61 μm , enabling bone microstructure to be evaluated with high accuracy. Unlike first-generation HR-pQCT, second-generation HR-pQCT enables direct measurement of trabecular bone microstructures [6].

Because human bone microstructure can be evaluated non-invasively without a bone biopsy by HR-pQCT, this

Electronic supplementary material The online version of this article (<https://doi.org/10.1007/s00774-020-01115-z>) contains supplementary material, which is available to authorized users.

✉ Ko Chiba
kohchiba@estate.ocn.ne.jp

¹ Department of Orthopedic Surgery, Nagasaki University Graduate School of Biomedical Sciences, 1-7-1 Sakamoto, Nagasaki 852-8501, Japan

method can be used to study age-related changes of bone microstructure in healthy populations. Although a number of previous studies have investigated them using first-generation HR-pQCT [7–9], few studies using second-generation HR-pQCT have yet been reported.

Microstructural parameters of trabecular bone include not only basic metric parameters such as trabecular thickness and separation, but also non-metric parameters such as the plate- or rod-like morphology of the trabeculae, trabecular connectivity, and trabecular anisotropy. These trabecular microstructures are expected to be deteriorated with advancing age. However, few HR-pQCT studies have examined such non-metric parameters.

The purpose of this study is to investigate deterioration of bone microstructure and strength by the aging and the menopause in healthy Japanese women by measuring trabecular and cortical bone microstructure including non-metric trabecular parameters and estimate bone strength using second-generation HR-pQCT.

Materials and methods

Participants

Study participants were 61 healthy Japanese female volunteers aged between 31 and 70 years (30–39 years: 16, 40–49 years: 20, 50–59 years: 16, 60–70 years: 11) who took part in the HR-pQCT study of healthy individuals (J-CaraT study: Japanese study of bone microstructure and mineral density in a non-medicative cohort measured by HR-pQCT) conducted at Nagasaki University between December 2015 and December 2016.

Individuals who had a history of disease or treatment with a medication that affected bone metabolism such as rheumatoid arthritis, kidney failure, liver failure, severe diabetes, hyperthyroidism, glucocorticoid therapy, hormone therapy, or treatment for malignancy, those with paralysis due to cerebral infarction or other condition were excluded from the study. In addition, pregnant, puerperal, and lactating women were also excluded.

This study was approved in advance by the Nagasaki University Hospital Clinical Research Ethics Committee (Approval Number: 15083105), and informed consent was obtained from all participants prior to enrolment.

DXA

DXA (Prodigy, GE Healthcare Systems, Wauwatosa, WI, USA) was used to measure areal bone mineral density (aBMD) and *T* score of the lumbar spine (L1–L4) and the proximal femur (total hip and femoral neck). All BMD

measurements were carried out by a single radiographer using the DXA equipment of a single institution.

HR-pQCT

Second-generation HR-pQCT (XtremeCT II, Scanco Medical AG, Brüttisellen, Switzerland) was used to scan the distal radius and tibia of the non-dominant arm and leg using the standard scanning protocol (voltage 68 kVp, tube current 1460 μ A, integration time 43 ms, number of projections 900, field of view 140 mm, matrix 2304 \times 2304, voxel size 60.7 μ m, total number of slices 168, scanning time 2 min, and effective dose 5 μ Sv). Reference lines were set at the hump on the wrist surface for the distal radius and the subchondral bone endplate of the distal-most part of the tibia for the distal tibia. An area 10.2-mm wide (164 slice images) was scanned at a point 9 mm proximal to the radial reference line and 22 mm proximal to the tibial reference line.

Motion artifacts were graded for all scans, and if motion artifacts that interfered with analysis were present, the scan was repeated. Motion artifacts were graded following the method described by Pialat et al. [10], and scans with grade 3–5 artifacts were excluded from analysis.

Bone microstructural analysis

Bone structure analysis software (TRI/3D-BON, Ratoc System Engineering Co. Ltd, Tokyo, Japan) was used to divide the bone into trabecular and cortical regions, and to analyze the bone microstructure of each region [11].

Trabecular bone analysis

Trabecular bone BMD (Tb.vBMD), bone volume fraction (BV/TV), trabecular number (Tb.N), trabecular thickness (Tb.Th), and trabecular separation (Tb.Sp) were evaluated in trabecular bone.

In this study, we also evaluated the non-metric parameters of structure model index (SMI), trabecular bone pattern factor (TbPf), connectivity density (Conn.D), number of nodes per cubic millimeter (N.Nd/TV), degree of anisotropy (DA), and star volume of marrow space (V*ms) (Supplementary Figure 1).

SMI is a three-dimensional parameter of trabecular morphology, with rod-like structures scored as 0, plate-like structures as 3, and mixtures of the two as intermediate values [12]. TbPf is another three-dimensional parameter of trabecular morphology, with honeycomb structures scored as negative values, plate-like structures as 0, and rod-like structures as positive values (Supplementary Figure 1) [13].

Conn.D is a parameter that evaluates trabecular connectivity, calculated from the number of cyclic structures formed by connections of trabeculae (bundle number, b1)

as $b1/TV$. A higher value indicates higher connectivity [14]. $N.Nd/TV$ is also a parameter that evaluates trabecular connectivity, and is calculated from the number of nodes in the skeletonized trabecular structure (Supplementary Figure 1). A higher value also indicates higher connectivity [15].

DA is a parameter that evaluates trabecular directionality by calculating anisotropy from the long and short axes of the mean intercept length (MIL) ellipse (long axis/short axis). A higher value indicates greater trabecular directionality [16].

V^*ms is a parameter that evaluates trabecular cavitation by measuring mean volume from an arbitrary point in the bone marrow to the point at which the cavity is cut off by trabeculae (Supplementary Figure 1). A higher value indicates more severe cavitation of the trabecular structure [17].

Cortical bone analysis

Cortical BMD (Ct.vBMD), cortical bone thickness (Ct.Th), cortical bone porosity (Ct.Po), average cortical bone pore volume (Ave Ct.Po.V), periosteal perimeter (Ps.Pm), and endocortical perimeter (Ec.Pm) were evaluated in cortical bone.

Estimated bone strength analysis

Estimated bone strength was evaluated with finite element analysis software (TRI/3D-FEM, Ratoc System Engineering Co.Ltd, Tokyo, Japan), using images of the distal radius and distal tibia.

Young's modulus was calculated from BMD values for each voxel, with Poisson's ratio as 0.3 [18]. Proximal planes of the distal radius and tibia were constrained, a compressive load corresponding to 10% distortion was applied from the distal to the proximal direction, and stiffness (kN/mm) was evaluated. Failure load (kN) was calculated with the bone breakdown condition defined as $\geq 0.7\%$ distortion and fracture defined as a breakdown rate of $\geq 7.5\%$ [19, 20].

Statistical analysis

Means and standard deviations were calculated for age, height, weight, body mass index (BMI), aBMD, T score, trabecular bone microstructure, cortical bone microstructure, and estimated bone strength.

To investigate age-related changes, Pearson's correlation coefficient between age and trabecular and cortical bone microstructure and estimated bone strength was analyzed. To investigate the effects of menopause on bone microstructure and strength during aging, interaction analysis was conducted. To investigate the factors that most affected the bone strength in trabecular and cortical bone microstructure, multiple linear regression analysis by the stepwise method was

performed. The level of statistical significance set at $p < 0.01$ (JMP pro ver.13, SAS Institute Inc, Cary, NC, USA).

Results

General characteristics of the participants are described in Table 1. Age ranged from 31 to 70 years. Mean height was 1.57 ± 0.05 m, mean weight was 54.4 ± 7.3 kg, and mean BMI was 22.0 ± 2.5 kg/m². Mean T scores on DXA were -0.59 ± 1.03 for the total hip, -0.80 ± 1.03 for the femoral neck, and -0.55 ± 1.50 for the lumbar spine (L1–4).

The aBMD values for the lumbar spine (L1–4), the total hip, and the femoral neck decreased with age (L1–4: $r = -0.39$, $p < 0.01$, total hip: $r = -0.36$, $p < 0.01$, femoral neck: $r = -0.44$, $p < 0.001$) (Fig. 1).

Motion artifacts in HR-pQCT images were grade 1 in 39 cases and grade 2 in 22 for the distal radius, and grade 1 in 52 cases and grade 2 in 9 for the distal tibia. All HR-pQCT images scanned in both distal radius and distal tibia could be used for the analysis of bone microstructures and strength ($n = 61$). Measurement values of trabecular and cortical bone microstructures and estimated bone strength are shown in Supplementary Table 1.

Trabecular bone

Correlations and interactions of trabecular bone parameters with age and menopause are shown in Table 2 and Fig. 2.

Tb.vBMD and BV/TV correlated negatively with age in the radius only ($r = -0.45$, $r = -0.48$) (Fig. 2a, b). Tb.N correlated negatively with age in both the radius and tibia ($r = -0.62$, $r = -0.46$) (Fig. 2c). Tb.Th correlated positively with age in the tibia ($r = 0.38$) (Fig. 2d). Tb.Sp and Tb.Sp.SD both showed positive correlations with age in both

Table 1 Background data of the participants

Variable	Whole cohort ($n = 61$)
Age (years)	48.3 ± 11.2 (31–70) 30–39 years: 16, 40–49 years: 20 50–59 years: 16, 60–70 years: 11
Post-menopause (n , %)	28 (45.9)
Age of menopause (years)	48.9 ± 5.5 (38–62)
Height (m)	1.58 ± 0.05 (1.41–1.69)
Weight (kg)	54.9 ± 7.4 (43–73)
Body mass index (kg/m ²)	22.1 ± 2.5 (17.6–27.8)
T score	
Lumbar spine (L1–4)	-0.55 ± 1.50 (–4.00–2.80)
Total hip	-0.59 ± 1.03 (–3.10–2.40)
Femoral neck	-0.80 ± 1.03 (–2.60–2.20)

Results are mean \pm SD (min–max)

Fig. 1 Scatter diagrams between age and aBMD measured by DXA. (Left) lumbar vertebrae L1-4, and (right) the total hip (orange plots: premenopausal women, blue plots: postmenopausal women)

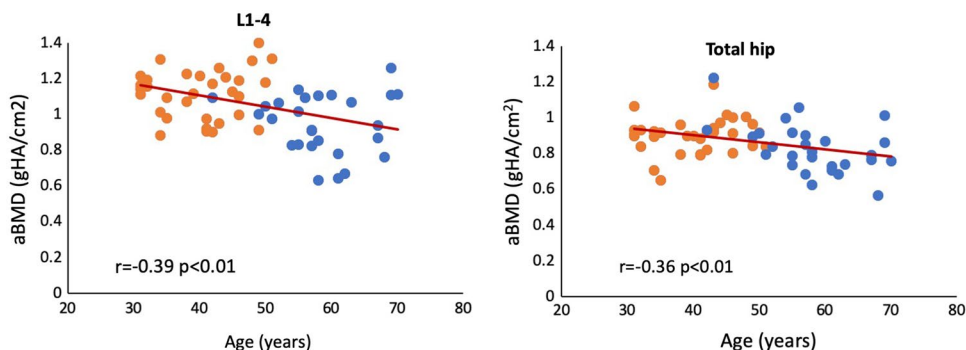


Table 2 Correlation and interaction analysis of trabecular and cortical bone microstructure and estimated bone strength with age and menopause

	Distal radius (N=61)			Distal tibia (N=61)		
	Correlation with age		Interaction with menopause	Correlation with age		Interaction with menopause
	r	p	p	r	p	p
Trabecular bone						
Tb.vBMD	-0.45	0.000**	0.045	-0.11	0.400	0.792
BV/TV	-0.48	0.000**	0.098	-0.19	0.149	0.596
Tb.N	-0.62	0.000**	0.409	-0.46	0.000**	0.533
Tb.Th	-0.05	0.687	0.003*	0.38	0.003*	0.802
Tb.Sp	0.60	0.000**	0.275	0.52	0.000**	0.479
Tb.Sp.SD	0.55	0.000**	0.007*	0.53	0.000**	0.718
SMI	0.38	0.002*	0.181	0.10	0.465	0.930
TBPf	0.33	0.001*	0.056	-0.02	0.893	0.989
Conn.D	-0.57	0.000**	0.761	-0.40	0.002*	0.862
N.Nd/TV	-0.59	0.000**	0.805	-0.42	0.001*	0.792
DA	-0.23	0.081	0.399	-0.08	0.533	0.940
V*ms	0.46	0.000**	0.074	0.41	0.001*	0.043
Cortical bone						
Ct.vBMD	-0.59	0.000**	0.011	-0.73	0.000**	0.009*
Ct.Th	-0.39	0.002*	0.000**	-0.52	0.000**	0.000**
Ct.Po	0.58	0.000**	0.741	0.61	0.000**	0.439
Ave Ct.Po.V	0.47	0.000**	0.907	0.32	0.013	0.741
Ps.Pm	0.23	0.078	0.308	0.17	0.194	0.387
Ec.Pm	0.27	0.035	0.789	0.30	0.019	0.904
Estimated bone strength						
Stiffness	-0.44	0.000**	0.000**	-0.54	0.000**	0.001*
Failure load	-0.44	0.000**	0.000**	-0.58	0.000**	0.001*

Pearson’s correlation coefficient, interaction analysis: * $p < 0.01$, ** $p < 0.001$

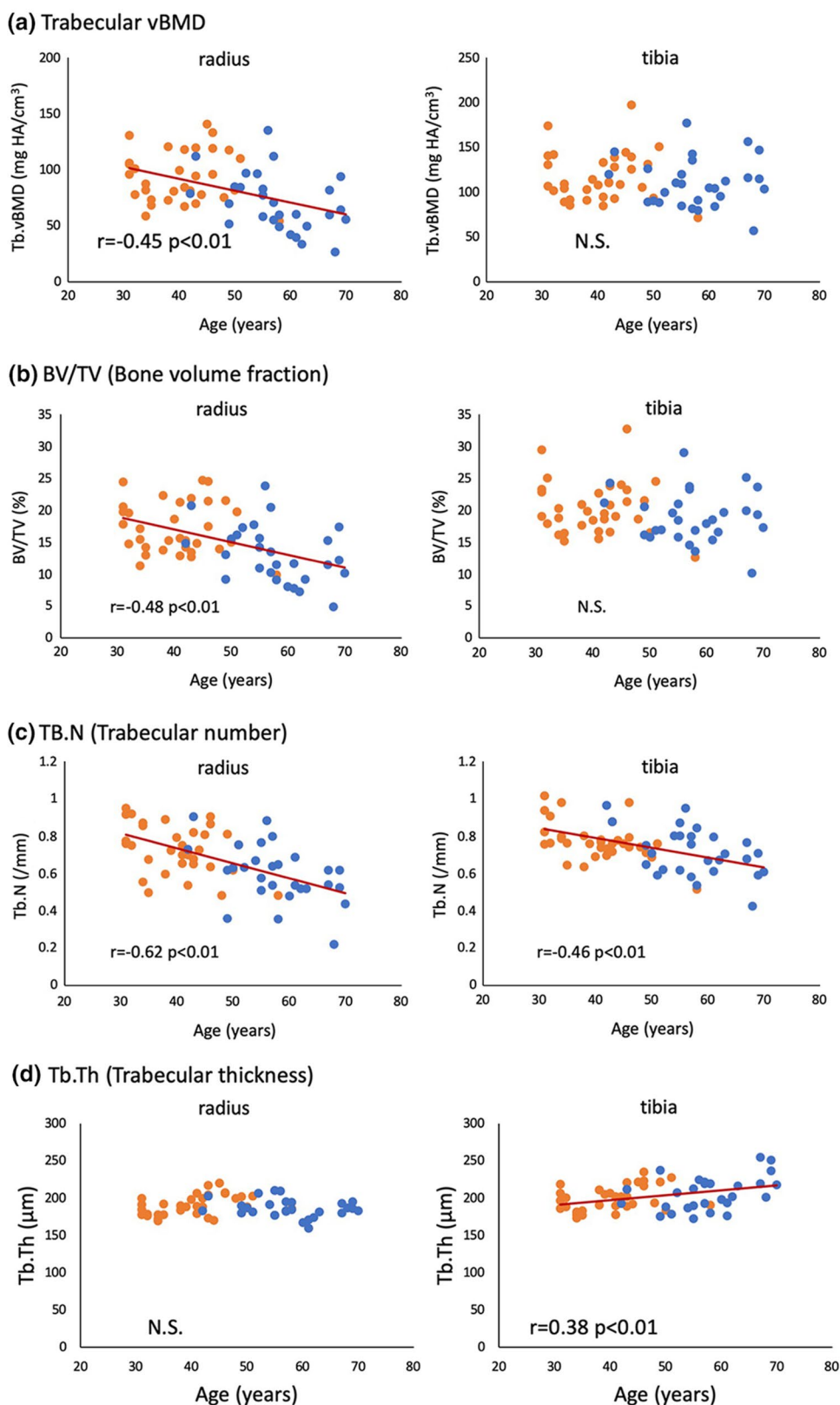
Tb.vBMD trabecular volumetric bone mineral density, BV/TV bone volume fraction, Tb.N trabecular number, Tb.Th trabecular thickness, Tb.Sp trabecular separation, Tb.Sp.SD standard deviation of trabecular separation, SMI structure model index, TBPf trabecular bone pattern factor, Conn.D connectivity density, N.Nd/TV number of node, DA degree of anisotropy, V*ms star volume of marrow space, Ct.vBMD cortical volumetric bone mineral density, Ct.Th cortical thickness, Ct.Po cortical porosity, Ave Ct.Po.V average cortical porosity volume, Ps.Pm periosteal perimeter, Ec.Pm endocortical perimeter

the radius and tibia (Tb.Sp: $r = 0.60$, $r = 0.52$) (Tb.Sp.SD: $r = 0.55$, $r = 0.53$) (Fig. 2e, f).

In terms of non-metric trabecular parameters, SMI and TBPf correlated positively with age in the radius only

($r = 0.38$, $r = 0.33$), meaning trabecular structure becoming increasingly rod-like (Fig. 2g, h). Conn.D and N.Nd/TV both correlated negatively with age in both the radius and

Fig. 2 Scatter diagrams between age and trabecular bone micro-structure. **a** Tb.vBMD, **b** BV/TV, **c** Tb.N, **d** Tb.Th, **e** Tb.Sp, **f** Tb.Sp.SD, **g** SMI, **h** TBPf, **i** Conn.D, **j** N.Nd/TV, **k** DA, and **l** V*ms in the distal radius and tibia (orange plots: premenopausal women, blue plots: postmenopausal women)



tibia (Conn.D: $r = -0.57$, $r = -0.40$) (N.Nd/TV: $r = -0.59$, $r = -0.42$), indicating a decline in trabecular connectivity (Fig. 2i, j). DA showed no correlations with age (Fig. 2k).

V*ms was positively correlated with age in both the radius and tibia ($r = 0.46$, 0.41), indicating progressive cavitation of the trabecular structure (Fig. 2l).

Fig. 2 (continued)

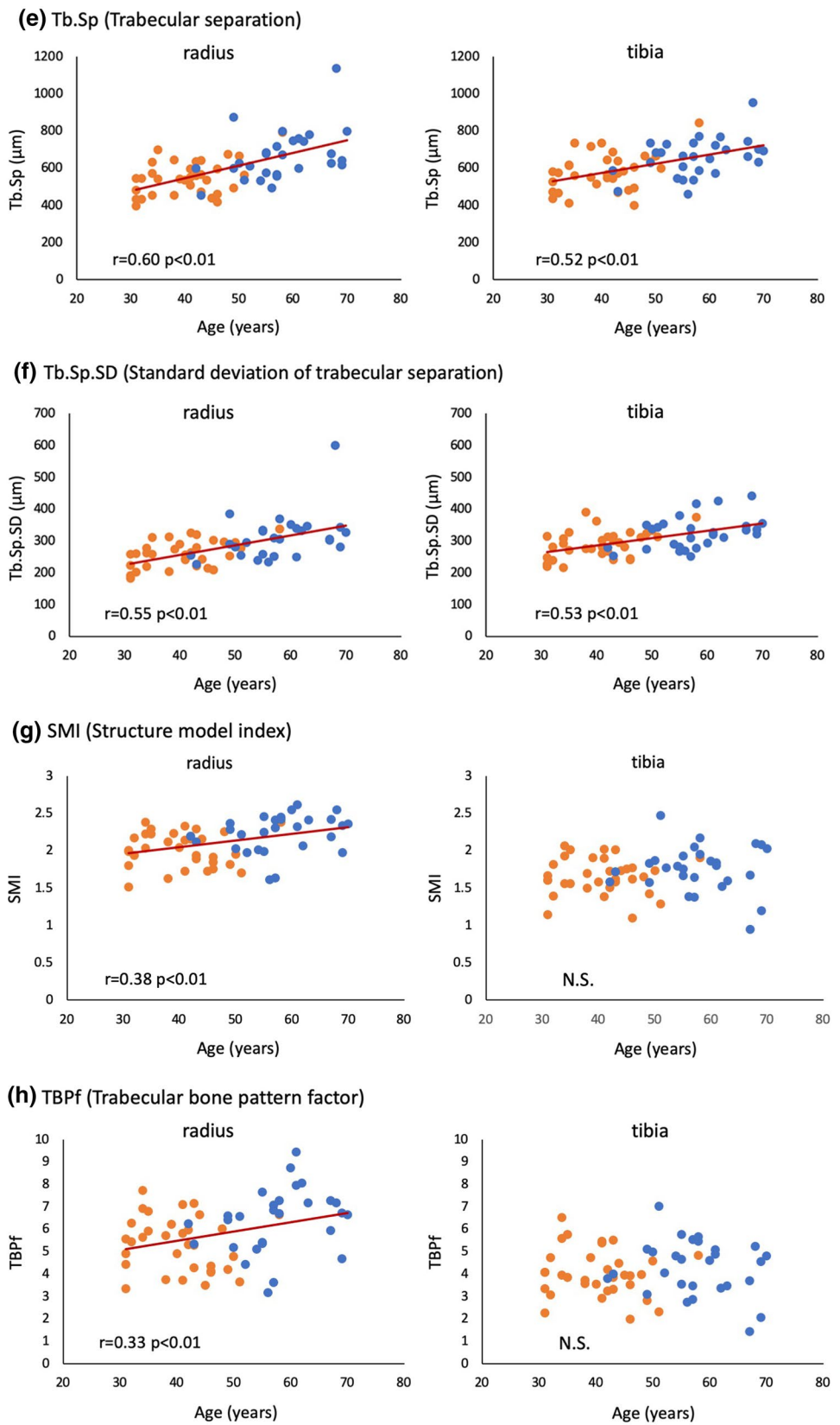


Fig. 2 (continued)

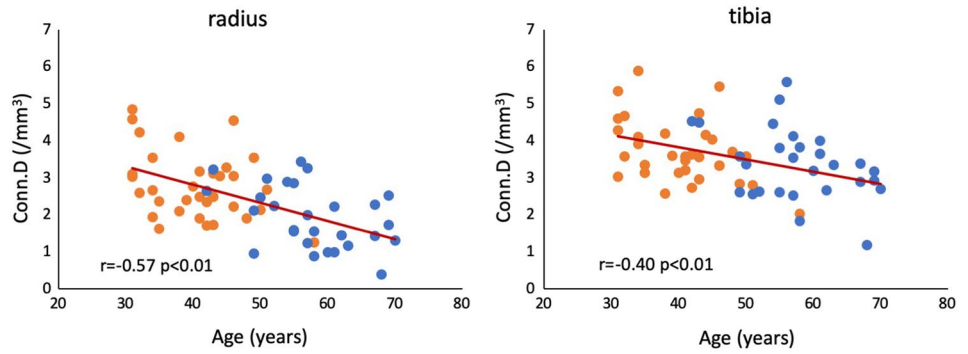
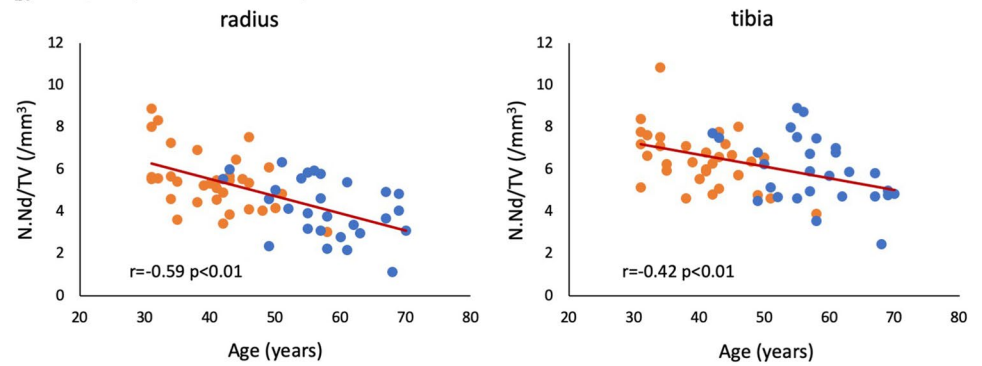
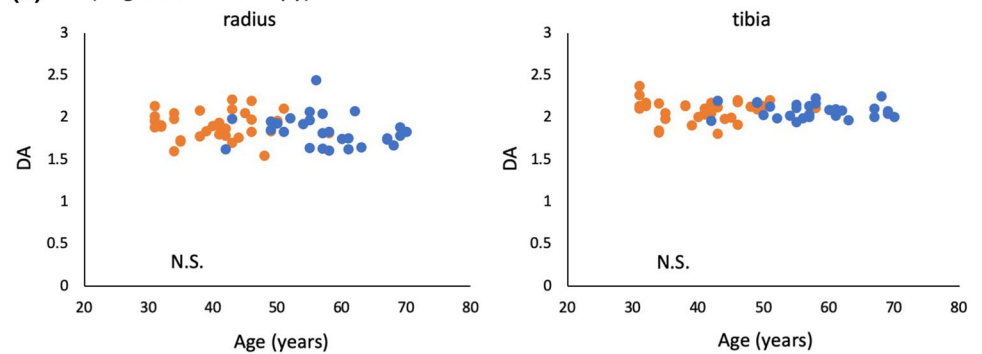
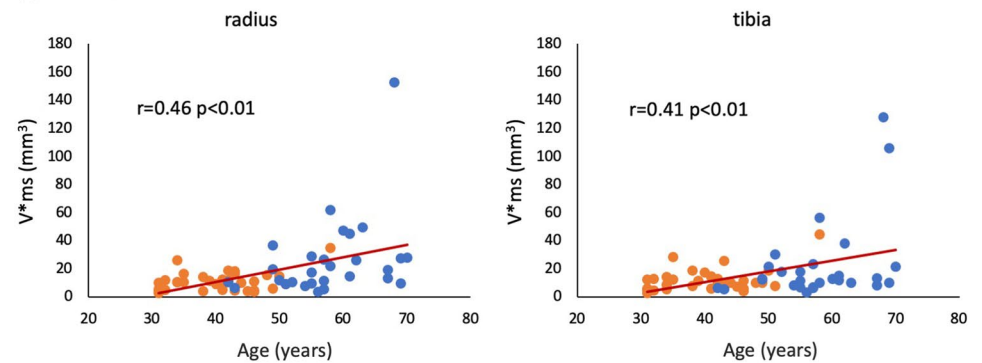
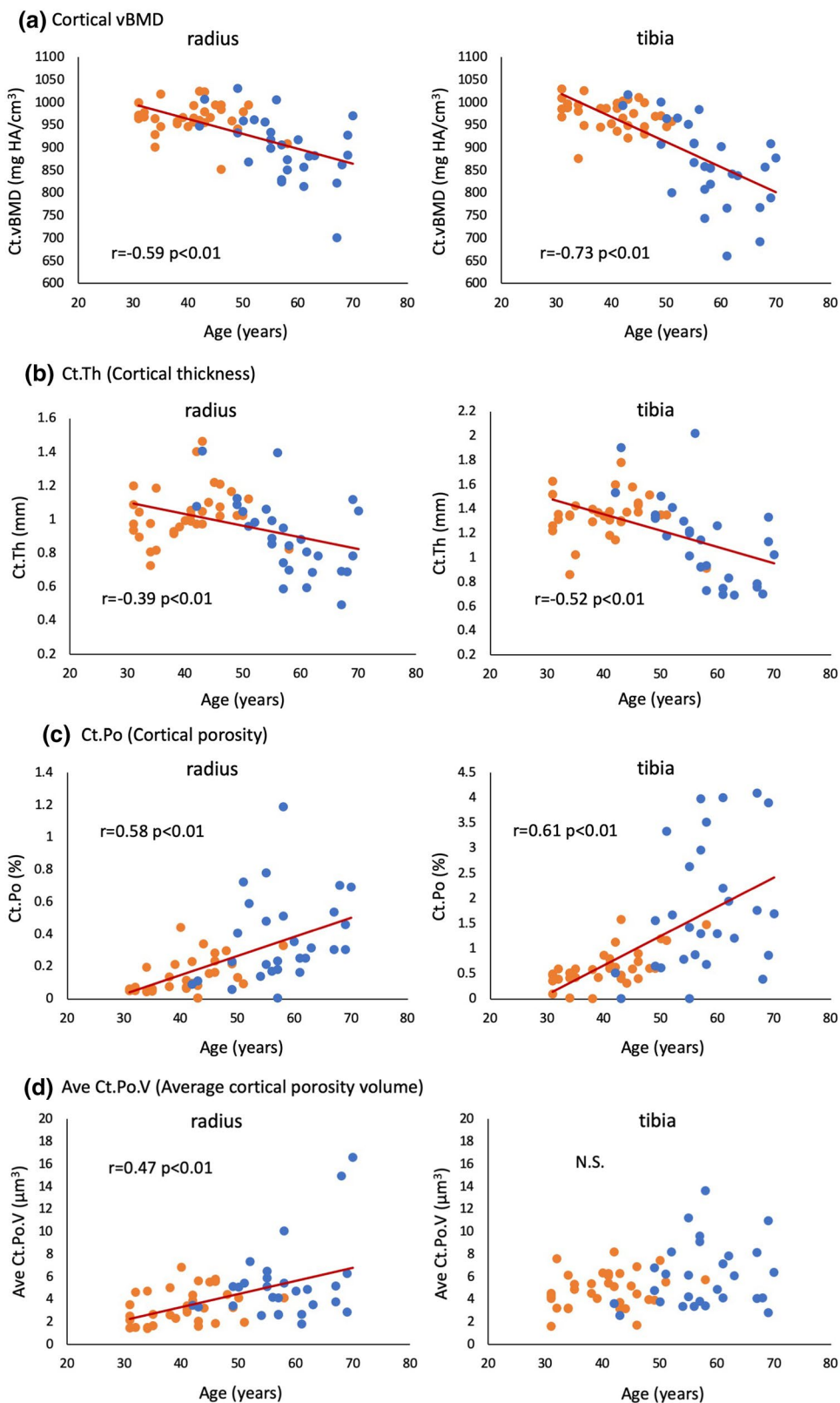
(i) Conn.D (Connectivity density)**(j) N.Nd/TV (Number of node)****(k) DA (degree of anisotropy)****(l) V*ms (Star volume of marrow space)**

Fig. 3 Scatter diagrams between age and cortical bone micro-structure. **a** Ct.vBMD, **b** Ct.Th, **c** Ct.Po, **d** Ave Ct.Po.V, **e** Ps.Pm, and **f** Ec.Pm in the distal radius and tibia (orange plots: premenopausal women, blue plots: postmenopausal women)



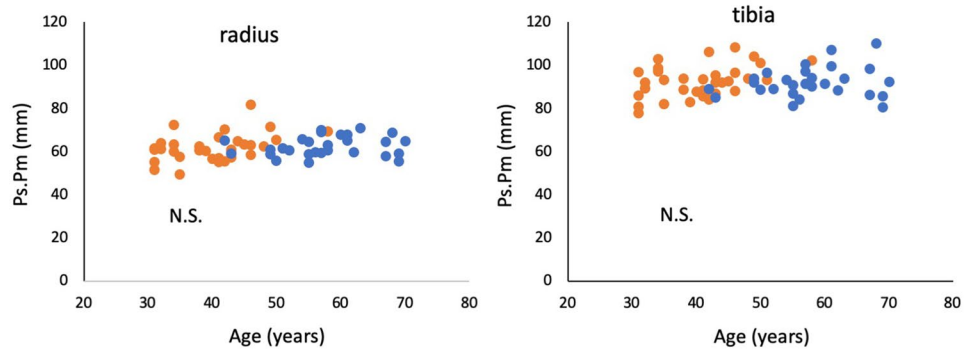
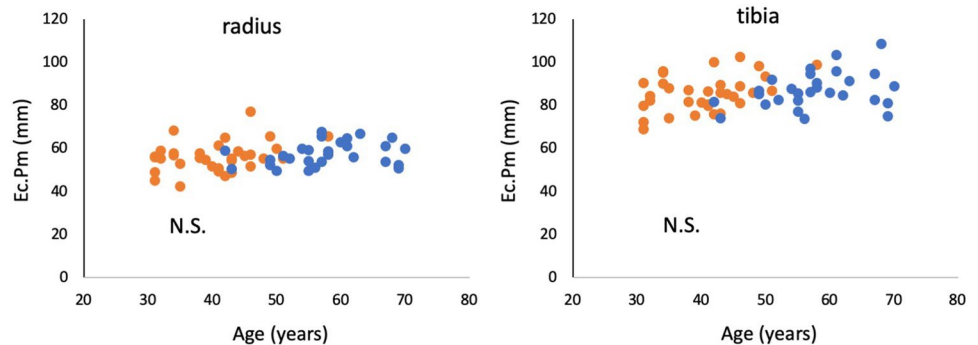
Cortical bone

Correlations and interactions of cortical bone parameters

with age and menopause are shown in Table 2 and Fig. 3.

Both Ct.vBMD and Ct.Th correlated negatively with age in both the radius and tibia (Ct.vBMD: $r = -0.59$, $r = -0.73$)

Fig. 3 (continued)

(e) Ps.Pm (Periosteal perimeter)**(f) Ec.Pm (Endocortical perimeter)**

(Ct.Th: $r = -0.39$, $r = -0.52$) (Fig. 3a, b). Ct.Po correlated positively with age in both the radius and tibia ($r = 0.58$, 0.61) (Fig. 3c), but Ave.Ct.Po.V was positively correlated with age in the radius only ($r = 0.47$) (Fig. 3d). Ps.Pm and Es.Pm were not correlated with age (Fig. 3e, f). Changes in Ct.Th and Ct.vBMD were significantly affected by menopause (Table 2).

Estimated bone strength

Correlations and interactions of estimated bone strength with age and menopause are shown in Table 2 and Fig. 4.

Both stiffness and failure load correlated negatively with age in both the radius and tibia (stiffness: $r = -0.44$, $r = -0.54$) (failure load: $r = -0.44$, $r = -0.58$), declining estimated bone strength with advancing age (Fig. 4a, b). These changes were significantly affected by menopause (Table 2).

Multiple linear regression analysis between estimated bone strength and trabecular and cortical bone microstructure are shown in Table 3. The most relevant factor of stiffness and FL was Ct.Th in both the radius and tibia.

Discussion

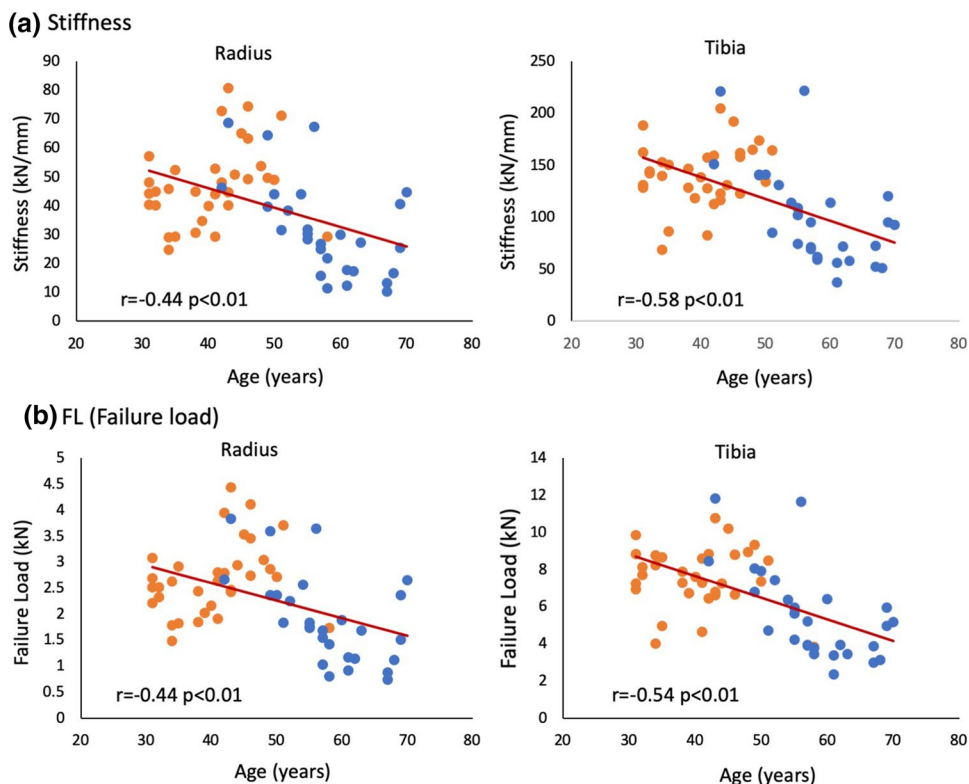
This study investigated age- and menopause-related changes in trabecular and cortical bone microstructures and estimated bone strength of healthy Japanese women using second-generation HR-pQCT.

The results showed that most of the trabecular and cortical bone microstructure and estimated bone strength deteriorated with age, and notably the decrease of Ct.Th, Ct.vBMD, stiffness, and FL was affected by menopause (Table 2; Figs. 2, 3, 4).

There were previous studies using first-generation HR-pQCT to investigate age-related changes in the bone microstructure and estimated bone strength of healthy populations. Those studies also reported the phenomenon that trabecular bone gradually decrease before menopause, whereas cortical bone and estimated bone strength were deteriorated rapidly after menopause [7–9].

The results also showed that Ct.Th is the most relevant factor of estimated bone strength (Table 3). It has been known that the deterioration of the cortical bone is caused by (1) bone loss on the inner surface of the cortical bone that leads to decreased Ct.Th and increased endocortical diameter, and (2) bone loss inside the cortical bone that leads to decreased Ct.vBMD and increased Ct.Po. This study showed particularly that decreased Ct.Th has the biggest impact to bone fragility.

Fig. 4 Scatter diagrams between age and estimated bone strength. **a** Stiffness and **b** failure load of the distal radius and tibia (orange plots: premenopausal women, blue plots: postmenopausal women)



Several studies have addressed the importance of cortical bone microstructure in terms of bone strength and fracture risk. Burghardt et al. showed that cortical porosity in women increased with advancing age and menopause, and that this was associated with a decrease in failure load analyzed by

the finite element method [21]. Sundh et al. reported that decreased cortical bone density and increased cortical porosity in the distal tibia were independent risk factors for proximal femoral fracture [22].

Table 3 Multiple linear regression analysis between estimated bone strength and trabecular and cortical bone microstructure

	<i>R</i>	β	<i>p</i>
(a) Distal radius			
Stiffness	0.924		0.000**
Ct.Th		0.725	0.000**
Tb.vBMD		0.305	0.000**
Failure load	0.921		0.000**
Ct.Th		0.760	0.000**
Tb.vBMD		0.256	0.000**
(b) Distal tibia			
Stiffness	0.966		0.000**
Ct.Th		0.754	0.000**
Ct.vBMD		0.210	0.001*
SMI		-0.156	0.000**
Failure load	0.966		0.000**
Ct.Th		0.632	0.000**
Ct.vBMD		0.305	0.000**
BV/TV		0.148	0.001*

Multiple linear regression analysis (stepwise): **p* < 0.01, ***p* < 0.001

Estimated bone strength analyzed by HR-pQCT is regarded as an important parameter for evaluating fragility fracture risk. Kroker et al. reported the correlation between failure load of the distal tibia analyzed by the finite element method using HR-pQCT images and the actual failure load of the proximal femur and lumbar vertebral body analyzed by mechanical testing, finding a stronger correlation between them than that of aBMD of the femur or lumbar spine as measured by DXA [23]. Samelson et al. conducted a meta-analysis of eight cohort studies, and reported that decreased failure loads of the distal radius and distal tibia as analyzed by the finite element method represented the most important risk factors for fragility fracture [24]. Frequencies of fragility fractures of the vertebral body and proximal femur in women obviously increase simultaneously with the decrease of estimated bone strength after menopause [25, 26].

We investigated detail of architectural changes in trabecular bone with advancing age and menopause by analyzing non-metric trabecular parameters. Both Conn.D and N.Nd/TV decreased with advancing age in both the distal radius and tibia, indicating a decline in trabecular connectivity (Fig. 2i, j). V*ms increased with advancing age, indicating increased trabecular cavitation (Fig. 2l). SMI and TBPf increased with advancing age in the distal radius only, with

trabecular structure becoming increasingly rod-like (Fig. 2g, h). However, DA did not change with age (Fig. 2k). Figure 5 shows images of the distal radius from a 42-year-old woman and a 68-year-old woman. The trabecular connectivity has been lost and cavitation is apparent with advancing age.

In the distal tibia, no changes were apparent in Tb.vBMD or BV/TV with advancing age (Fig. 2a, b). There was a possibility that the distal tibia exhibited fewer age-related changes in bone microstructure compared with the distal radius because of its nature as a weight-bearing bone. However, age-related changes in Conn.D, N.Nd/TV, and V*ms were also evident in the distal tibia (Fig. 2i–l). This might represent the earlier detection of osteoporotic changes in trabecular structures.

Sornay-Rendu et al. compared subjects with a history of osteoporotic fragility fracture to those who did not have the history, and reported that Conn.D declined and SMI was high (rod-like) among subjects with osteoporotic fragility fracture [27]. In this study, non-metric trabecular parameters provided an additional information for assessing a risk of osteoporotic fragility fracture.

Thus, evaluations that combine conventional metric trabecular parameters with the non-metric trabecular

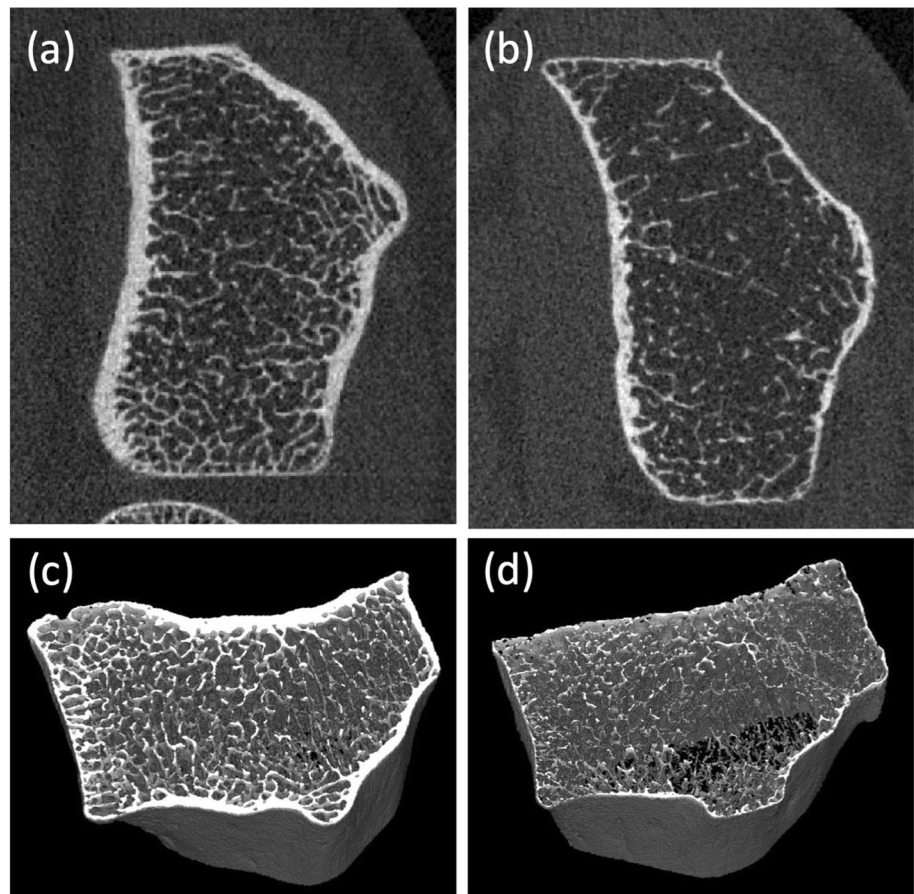
parameters may provide useful information for the clinical assessment of osteoporosis.

Limitations

This study had a number of limitations. The first was that the participants were limited to 61 healthy Japanese women. The small scale of the study means that it cannot be said to represent all age-related changes that occur in women, and the findings should rather be regarded as exploratory results. The second was its nature as a cross-sectional study. Although we investigated changes due to advancing age and menopause, these do not provide a full understanding of osteoporotic changes over time. High-quality prospective studies are required to clarify age-related changes in bone microstructure and estimated bone strength. The J-CaraT study will eventually comprise a prospective study of data from 520 healthy volunteers between 20 and 89 years, and further reports including additional data will be published in the future.

In conclusion, we investigated age-related changes and the effect of menopause on trabecular and cortical bone

Fig. 5 HR-pQCT images of the distal radius of **a** a 42-year-old woman and **b** a 68-year-old woman. In addition to thinning of the cortical bone, osteoporotic changes to the trabecular bone are apparent with a decrease of the connectivity and increase of the cavitation (Conn.D: 1.71/mm³ vs 0.40/mm³, N.Nd/TV: 3.44/mm³ vs 1.14/mm³, V*ms: 18.8 mm³ vs 152.6 mm³)



microstructure and estimated bone strength in healthy Japanese women using second-generation HR-pQCT. Trabecular and cortical bone microstructures and estimated bone strength exhibited major changes due to advancing age and menopause. Age-related changes in non-metric trabecular parameters were clearly evident, suggesting that these may represent useful parameters for evaluating osteoporotic changes in trabecular three-dimensional structures.

Acknowledgements We would like to thank Shuntaro Sato, a specialist in biostatistics, for providing advice on the statistical analyses, and Nobuhito Nango, a developer of bone measurement software, for advising bone microstructural analysis.

Author contributions Study design: KC; data acquisition: KY, NO, CK, MD, SY, ME, and YN; data analysis: KY and KC; data interpretation: KY and KC; drafting of the manuscript: KY; revision of manuscript content: KC and MO; approval of the final version of the manuscript: KY, KC, AY, MT, and MO.

Compliance with ethical standards

Conflict of interest The authors declare that they have no conflict of interest.

References

- Stone KL, Seeley DG, Lui L-Y, Cauley JA, Ensrud K, Browner WS, Nevitt MC, Cummings SR (2003) BMD at multiple sites and risk of fracture of multiple types: long-term results from the study of osteoporotic fractures. *J Bone Miner Res* 18:1947–1954
- Delmas PD, Seeman E (2004) Changes in bone mineral density explain little of the reduction in vertebral or nonvertebral fracture risk with anti-resorptive therapy. *Bone* 34:599–604
- Burghardt AJ, Link TM, Majumdar S (2011) High-resolution computed tomography for clinical imaging of bone microarchitecture. *Clin Orthop Relat Res* 469:2179–2193
- Nishiyama KK, Shane E (2013) Clinical imaging of bone microarchitecture with HR-pQCT. *Curr Osteoporos Rep* 11:147–155
- Cheung AM, Adachi JD, Hanley DA, Kendler DL, Davison KS, Josse R, Brown JP, Ste-Marie L-G, Kremer R, Erlandson MC, Dian L, Burghardt AJ, Boyd SK (2013) High-resolution peripheral quantitative computed tomography for the assessment of bone strength and structure: a review by the Canadian bone strength working group. *Curr Osteoporos Rep* 11:136–146
- Manske SL, Zhu Y, Sandino C, Boyd SK (2015) Human trabecular bone microarchitecture can be assessed independently of density with second generation HR-pQCT. *Bone* 79:213–221
- Hansen S, Shanbhogue V, Folkestad L, Nielsen MMF, Brixen K (2013) Bone microarchitecture and estimated strength in 499 adult Danish women and men: a cross-sectional, population-based high-resolution peripheral quantitative computed tomographic study on peak bone structure. *Calcif Tissue Int* 94:269–281
- Hung VWY, Zhu TY, Cheung WH, Fong TN, Yu FWP, Hung LK, Leung KS, Cheng JCY, Lam TP, Qin L (2015) Age-related differences in volumetric bone mineral density, microarchitecture, and bone strength of distal radius and tibia in Chinese women: a high-resolution pQCT reference database study. *Osteoporos Int* 26:1691–1703
- Vilayphiou N, Boutroy S, Sornay-Rendu E, Van Rietbergen B, Chapurlat R (2016) Age-related changes in bone strength from HR-pQCT derived microarchitectural parameters with an emphasis on the role of cortical porosity. *Bone* 83:233–240
- Pialat JB, Burghardt AJ, Sode M, Link TM, Majumdar S (2012) Visual grading of motion induced image degradation in high resolution peripheral computed tomography: Impact of image quality on measures of bone density and micro-architecture. *Bone* 50:111–118
- Nango N, Takeuchi N (1997) 3D image processing technology. *Metal* 67:653–663 (in Japanese)
- Hildebrand T, Rüegsegger P (1997) Quantification of bone microarchitecture with the structure model index. *Comput Methods Biomech Biomed Eng* 1:15–23
- Hahn M, Vogel M, Pompesius-Kempa M, Delling G (1992) Trabecular bone pattern factor—a new parameter for simple quantification of bone microarchitecture. *Bone* 13:327–330
- Odgaard A, Gundersen HJG (1993) Quantification of connectivity in cancellous bone, with special emphasis on 3-D reconstructions. *Bone* 14:173–182
- Mellish RWE, Ferguson-Pell MW, Cochran GVB, Lindsay R, Dempster DW (1991) A new manual method for assessing two-dimensional cancellous bone structure: comparison between iliac crest and lumbar vertebra. *J Bone Miner Res* 6:689–696
- Hildebrand T, Rüegsegger PR (1997) A new method for the model-independent assessment of thickness in three-dimensional images. *J Microsc* 185:1–9
- Vesterby A, Gundersen HJG, Melsen F (1989) Star volume of marrow space and trabeculae of the first lumbar vertebra: Sampling efficiency and biological variation. *Bone* 10:7–13
- MacNeil JA, Boyd SK (2008) Bone strength at the distal radius can be estimated from high-resolution peripheral quantitative computed tomography and the finite element method. *Bone* 42:1203–1213
- Boutroy S, Van Rietbergen B, Sornay-Rendu E, Munoz F, Bouxsein ML, Delmas PD (2007) Finite element analysis based on in vivo HR-pQCT images of the distal radius is associated with wrist fracture in postmenopausal women. *J Bone Miner Res* 23:392–399
- Pistoia W, van Rietbergen B, Lochmüller EM, Lill CA, Eckstein F, Rüegsegger P (2002) Estimation of distal radius failure load with micro-finite element analysis models based on three-dimensional peripheral quantitative computed tomography images. *Bone* 30:842–848
- Burghardt AJ, Kazakia GJ, Ramachandran S, Link TM, Majumdar S (2009) Age and gender related differences in the geometric properties and biomechanical significance of intra-cortical porosity in the distal radius and tibia. *J Bone Miner Res* 25:983–993
- Sundh D, Nilsson AG, Nilsson M, Johansson L, Mellström D, Lorentzon M (2017) Increased cortical porosity in women with hip fracture. *J Intern Med* 281:496–506
- Kroker A, Plett R, Nishiyama KK, McErlain DD, Sandino C, Boyd SK (2017) Distal skeletal tibia assessed by HR-pQCT is highly correlated with femoral and lumbar vertebra failure loads. *J Biomech* 59:43–49
- Samelson EJ, Broe KE, Xu H, Yang L, Boyd S, Biver E, Szulc P, Adachi J, Amin S, Atkinson E, Berger C, Burt L, Chapurlat R, Chevalley T, Ferrari S, Goltzman D, Hanley DA, Hannan MT, Khosla S, Liu C-T, Lorentzon M, Mellstrom D, Merle B, Nethander M, Rizzoli R, Sornay-Rendu E, Van Rietbergen B, Sundh D, Wong AKO, Ohlsson C, Demissie S, Kiel DP, Bouxsein ML (2019) Cortical and trabecular bone microarchitecture as an independent predictor of incident fracture risk in older women and men in the Bone Microarchitecture International Consortium (BoMIC): a prospective study. *Lancet Diabetes Endocrinol* 7:34–43
- Tamaki J, Fujimori K, Ikehara S, Kamiya K, Nakatoh S, Okimoto N, Ogawa S, Ishii S, Iki M (2019) Estimates of hip fracture

- incidence in Japan using the National Health Insurance Claim Database in 2012–2015. *Osteoporos Int* 30:975–983
26. Yoshimura N, Kinoshita H, Oka H, Muraki S, Mabuchi A, Kawaguchi H, Nakamura K (2006) Cumulative incidence and changes in the prevalence of vertebral fractures in a rural Japanese community: a 10-year follow-up of the Miyama cohort. *Arch Osteoporos* 1:43–49
27. Sornay-Rendu E, Boutroy S, Duboeuf F, Chapurlat RD (2017) Bone microarchitecture assessed by HR-pQCT as predictor of fracture risk in postmenopausal women: the OFELY study. *J Bone Miner Res* 32:1243–1251

Publisher's Note Springer Nature remains neutral with regard to jurisdictional claims in published maps and institutional affiliations.